A STUDY OF A CHARACTERISTIC TPYE OF UPPER-LEVEL FRONTOGENESIS

By Richard J. Reed

Massachusetts Institute of Technology [1,2]

(Manuscript received 10 August 1954)

ABSTRACT

The potential vorticity on isentropic surfaces is used to study a characteristic type of upper-level frontogenesis — the development of a sloping stable layer marked by strong vertical wind shear and rapid upward decrease in humidity. In the case studied it was found that the intense portion of the frontal zone consisted of a thin wedge of stratospheric air which had descended to very low levels (700 to 800 millibars), the frontal boundaries being a folded portion of the original tropopause.

The circulation within the frontal zone was indirect solenoidal, and surface cyclogenesis accompanied or slightly preceded the strengthening of the upper-level front. Although the frontal zone formed entirely within a polar air-mass, the strong adiabatic heating at and near the warm boundary could give the false impression that tropical air was present there at the end stage.

1. Introduction

From a detailed study of surface weather-elements and simultaneous observation of the sky, J. Bjerknes (1919) concluded that the extratropical cyclone contains two principal lines of convergence which meet at the low-pressure center and mark the boundary of a region of warm air or "warm sector." Subsequent refinement and expansion of this cyclone model by Bjerknes and Solberg (1922) and Bergeron (1928) provided the empirical background for the revolutionary wave theory of cyclones. According to this theory, the extratropical low forms as a wave disturbance on a relatively sharp, sloping boundary surface separating tropical and polar air-masses. This boundary surface — the polar front — is the seat of the shearing instability which gives raise to the disturbance, and is also the source of the solenoidal energy which is transformed into kinetic energy as the storm intensifies. For theoretical purposes, at least, it was felt that the front could be treated as a zero-order discontinuity in temperature (or density), and, in the absence of upper-air data, it was assumed from cloud observation that the temperature discontinuity extended to the upper troposphere.

When the introduction of upper-air soundings made possible direct observation of cyclonic structure in the free atmosphere, no evidence of the assumed temperature discontinuity was found. However, there were on certain soundings abrupt changes in temperature lapse-rate which led Bjerknes (1929) to observe that frontal discontinuities aloft are of the first order, that is, that they are discontinuities in temperature gradient rather than temperature itself. Thus the concept of a frontal surface was replaced by that of a frontal zone, and, on upper-level charts or in vertical cross-sections, either a single line was used to denote the boundary between tropical and transitional air or else two lines were drawn separating the polar and tropical air-masses from a zone of transition.

Minor modifications and refinements of the early cyclone model have appeared in later years, but the basic features remain unchanged, and it is still the universal partice to analyze and describe weather situations in conformity with the classical model. However, with the vast accumulation of weather data — surface and upper air — during the past twenty years, it has become increasingly apparent that the thermal structure of cyclones is in general considerably more complex and diffuse than was visualized by the Norwegian school. In fact, in continential areas where observational data are plentiful, cases in which storms form on sharp, preexisting fronts separating air of distinctly polar and tropical origin are the exception rather than the rule. Realizing such discrepancies between observation and theory, many forecasters have tended to become skeptical of the classical model; yet, in deference to convention, they continue to enter the ideal fronts on surface weather-charts, even when there is little empirical basis for the analysis.

The theoretical meteorologist, on the other hand, has in recent years abandoned the concept of an atmosphere containing discontinuities in temperature or temperature gradient and has tended to think more and more in terms of a continuous medium characterized by broad zones of relatively strong

[1] The research reported in this article was sponsored by the Office of Naval Research, under Contract No. N5ori-07804, between the Office of Naval Research and the Division of Industrial Cooperation, Massachusetts Institute of Technology.

[2] Present affiliation: University of Washington.

temperature concentration. The comparative fruitfulness of this approach in problems relating to the stability of baroclinic zonal currents and the numerical prediction of pressure or height changes has raised justifiable doubts as to whether fronts play a leading role in atmospheric developments. Sutcliffe (1952), in a review article which expresses opinions similar to the foregoing, has emphasized the present uncertain position of the frontal concept. However, he has also stated, and correctly, that "for some reason, not so far as we know yet adequately explained, the baroclinic atmosphere does frequently develop towards discontinuity in temperature, often very sharp near the surface, and the field of vertical motion, in the lower troposphere at least, does tend to organize itself in gentle upsliding motions in these regions." Since, as stressed by Palmén (1949), there are instances of distinct fronts in the upper troposphere, there appears no reason for restricting the preceding statement to the lower troposphere. Godson (1951) has suggested the term "hyperbaroclinic zone" for the sharply bounded zone of temperature concentration and "frontal zone" for the broad baroclinic region without distinct boundaries. The writer, however, prefers to refer to baroclinic zones as such and to reserve the designation "frontal zone" for the narrow, sharply bounded region of intense temperature contrast. The latter terminology will be employed in this article.

In the present state of affairs, it is not likely that clarification of the frontal problem will come from further refinement of the classical model. Instead, what is needed is a reexamination of the whole subject from a fresh viewpoint. The first step in such a reappraisal is to recognize that many "fronts" are merely zones of relatively strong temperature contrast without significant discontinuities in temperature or temperature gradient; and although it may be convenient to refer to such zones as frontal zones,

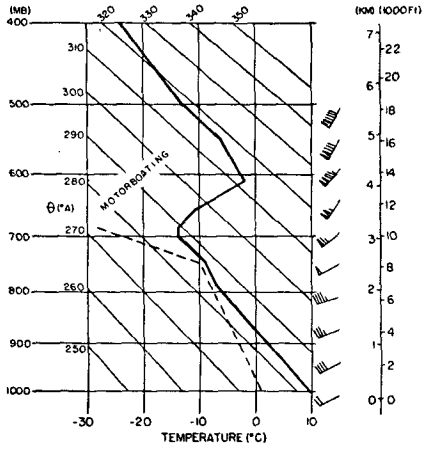

FIG. 1. Upper-air sounding for Norfolk, Va., 0300 GCT 15 December 1953. Temperature curve, solid line; dew-point curve, dashed line. Each half barb represents wind speed of 5 kn, full barb 10 kn, and solid wedge 50 kn. "Motorboating" indicates humidity too low to be measured.

there is little to be gained by marking them in a special manner on maps or in cross sections. In such cases, the temperature field should be allowed to speak for itself. The second step is to recognize that true frontal zones do appear frequently in the atmosphere in conncection with cyclonic development, and that they are not all necessarily of the same character and origin. It then becomes a main task of frontal theory to describe and explain the origin and behavior of the various kinds of frontal zones that observation reveals.

Proceeding from this point of view, Sanders (1954) has distinguished, on the basis of a number of case studies, two main types of frontal zones. The first of these reaches its greatest intensity near the ground and generally becomes diffuse above the 700-mb level. It is characterized by rising motion within a relatively narrow layer which slopes upward from an elongated zone of convergence at the earth's surface. The second type of frontal zone attains its greatest strength, as a rule, in middle portions of the troposphere. It is similar to or identical with the "katafront" or subsiding cold front, first noted by Bergeron (1937) and more recently studied by Sansom (1952). Presented in fig. 1 is a sounding through an unusually pronounced, but typical katafront, showing the characteristic rapid upward decrease in humidity within a thin stable layer of strong vertical wind shear.

The development of a representative katafront has been investigated recently by Reed and Sanders (1953), in an article in which they treat the thermal and vorticity aspects of the frontogenesis separately. The present article is an extension of this earlier work. It deals with a much more remarkable case of frontal development, and, because of the location of the final frontal zone, the development can be traced over a considerably longer time interval and larger geographical area. But more importantly, the present investigation makes use of a different and, insofar as fronts are concerned, a new method of analysis which it is felt has definite advantages for the problem at hand. This method, which utilizes the potential vorticity on isentropic surfaces, was outlined and illustrated in the previous article but was not applied to the overall development. Stated briefly, then, the primary purpose of the present article is to study the formation of a particular type of frontal zone by means of a technique involving the potential vorticity.

From fig. 1, it is apparent that the katafront studied here is of an intensity rarely encountered in atmospheric soundings. It may be argued, therefore, that the case under consideration is a freak and that conclusions based upon it are of little general interest. However, the writer takes the position that the unusual intensity does not necessarily indicate that an

unusual process was in operation, but more likely that a common process acted with unusual vigor. The selection of an extreme development has the advantage of making easier the procurement of reliable measurements and the interpretation of the measurements. It is felt that this advantage outweighs any disadvantages resulting from a possible loss of generality.

2. Basic equations and method of application

According to a conservation theorem first derived by Ertel (1942), the following relationship holds for adiabatic, frictionless motion:

$$\frac{d}{dt}[\sigma(\nabla \times V + 2\Omega)\cdot\nabla\theta] = 0. \qquad (1)$$

In this equation, σ is the specific volume, $\Delta \times V$ the three-dimensional relative vorticity, Ω the earth's rotation vector, and $\nabla\theta$ is the three-dimensional potential-temperature gradient. By a transformation of coordinates, it can be shown that, to a high degree of approximation, (1) may be written as

$$(\zeta_\theta + f)\,\partial\theta/\partial p = P, \qquad (2)$$

where $\zeta_\theta = (\partial v/\partial x - \partial u/\partial y)_\theta$, the vorticity measured from horizontal wind components on a potential-temperature surface, f is the Coriolis parameter, and P is a constant following the motion of the individual air particle but varying from one particle to the next. Alternatively, (1) may be written as

$$(\zeta_p + f)\frac{\partial\theta}{\partial p} + K\cdot\frac{\partial V_2}{\partial p} \times \nabla_p\theta = P. \qquad (3)$$

In (3), $\zeta_p = (\partial v/\partial x - \partial u/\partial y)_p$, the vorticity measured on a constant-pressure surface, K is the unit vertical vector, V_2 the horizontal wind vector, and $\nabla_p\theta$ is the potential-temperature gradient on the constant-pressure surface.

The first term in (3) is frequently referred to as the potential vorticity or potential absolute vorticity. However, since in zones of strong temperature contrast the second term is of appreciable magnitude, the total expression is significantly more conservative than its components. For this reason, it seems preferable to denote the quantity P in (2) and (3) as the potential vorticity, and the quantity $(\zeta_p + f)(\partial\theta/\partial p) = P'$ as the partial potential vorticity. This convention has been adopted in the present article.

Equation (3) relates the variations of absolute vorticity, thermal stability, vertical wind shear and horizontal potential-temperature gradient that accompany the motion of an individual air particle and, therefore, provides a means of relating frontogenesis (by definition an increase in $\nabla_p\theta$) to significant dynamic and thermal parameters. By studying or "explaining" frontogenesis, it is meant here (a) that the history of air particles within the frontal zone is traced, with use of the potential vorticity as an identifier, and (b) that the increase in horizontal temperature gradient on these particles is shown to be consistent with the changes in the other variables in (3).

In accordance with this treatment of the frontogenetical problem, there are two steps in the procedure:

1. Equation (2) is utilized to measure the potential vorticity at successive synoptic hours on selected isentropic surfaces; it is

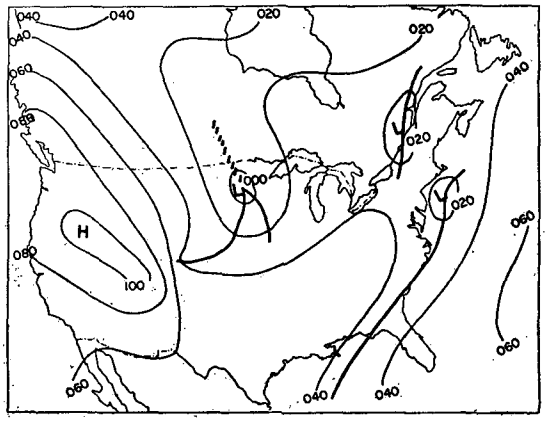

FIG. 2. 1000-mb surface for 0300 GCT 13 December 1953. showing contours (thin solid lines) and fronts (heavy solid lines), Contour height in feet.

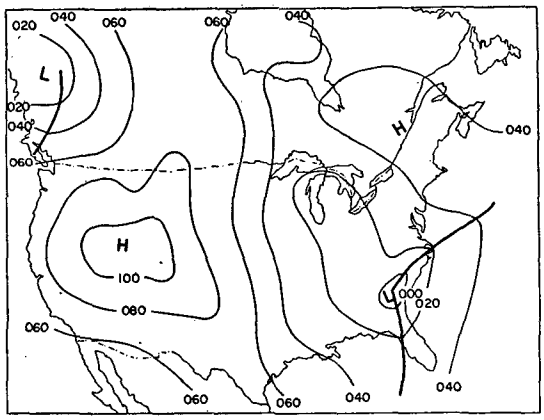

FIG. 3. 1000-mb surface for 0300 GCT 14 December 1953.

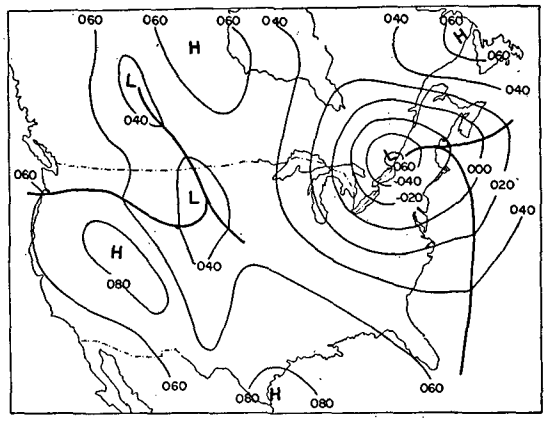

FIG. 4. 1000-mb surface for 0300 GCT 15 December 1953.

essential to work on isentropic surfaces, to take into account the vertical component of motion;

2. The parameters in (3) are evaluated at the same hours along the same isentropic surfaces; however, since it is difficult to measure all of these directly on an isentropic surface, it has been necessary to resort to an indirect method described in the appendix. Suffice it to say at this point that in this method the second term in (3) is determined by assuming that the thermal-wind relationship holds, $\partial V_2/\partial p \approx \nabla_p \theta$; and the first term, the partial potential vorticity, is found by subtracting the second term from P, the potential vorticity. In order that the vorticity, ζ_p, may be considered an independent parameter, spot checks were made between derived and directly measured values.

3. The case of 13–15 December 1953

The remarkable frontogenesis which forms the subject of the present article took place mainly between 0300 GCT 14 December and 0300 GCT 15 December 1953. However, sufficient data are available to trace weather events back an additional 24 hr, and therefore nearly all charts have been prepared at the five synoptic hours: 0300 and 1500 GCT 13 December, 0300 and 1500 GCT 14 December, and 0300 GCT 15 December. Because of space considerations, only a limited number of these charts is presented here.

Shown first, in figs. 2 to 4, are the 1000-mb charts for 0300 GCT on the 13th, 14th and 15th. At the initial time, a quasi-stationary front was located over the southeastern United States with a weak suggestion of a wave in the Gulf of Mexico. Also present over the United States was an Alberta-type low, moving southeastward across the northern Great Plains. This disturbance was a remnant of an intense cyclone which had earlier been in the Gulf of Alaska. During the next 24 hr the two pressure systems merged, the Alberta low filling in the process and the wave in the southeast undergoing considerable deepening. Meanwhile, the cold front accompanying the Alberta low became indistinct. Between 0300 GCT 14 December and 0300 GCT 15 December, the period of intense frontogenesis aloft, the surface cyclone moved northward to a position near Lake Ontario and deepened by approximately 600 ft (21 mb).

Developments at the 500-mb level are shown in figs. 5 to 7. Initially (fig. 5), a weak cold low was present in southern Texas in connection with the wave in the Gulf of Mexico. There was little evidence of any upper-level trough accompanying the A berta low. However, there was a zone of cyclonic shear over western Canada, and a mass of extremely cold air possessing cyclonic thermal vorticity in this same region. During the following 24 hr, a strong trough

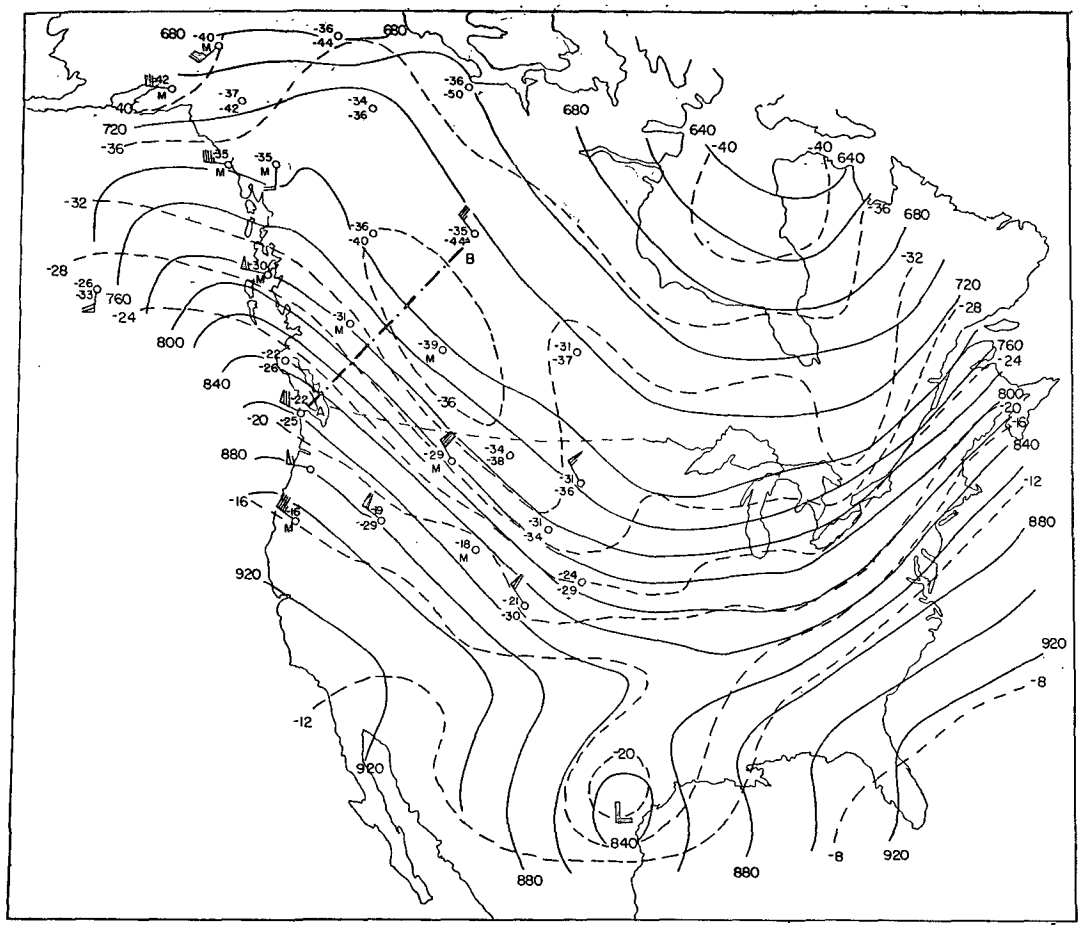

FIG. 5. 500-mb surface for 0300 GCT 13 December 1953, showing contours (thin solid lines) and isotherms (thin dashed lines). Observed temperatures and dew points (deg C) and winds added in critical areas.

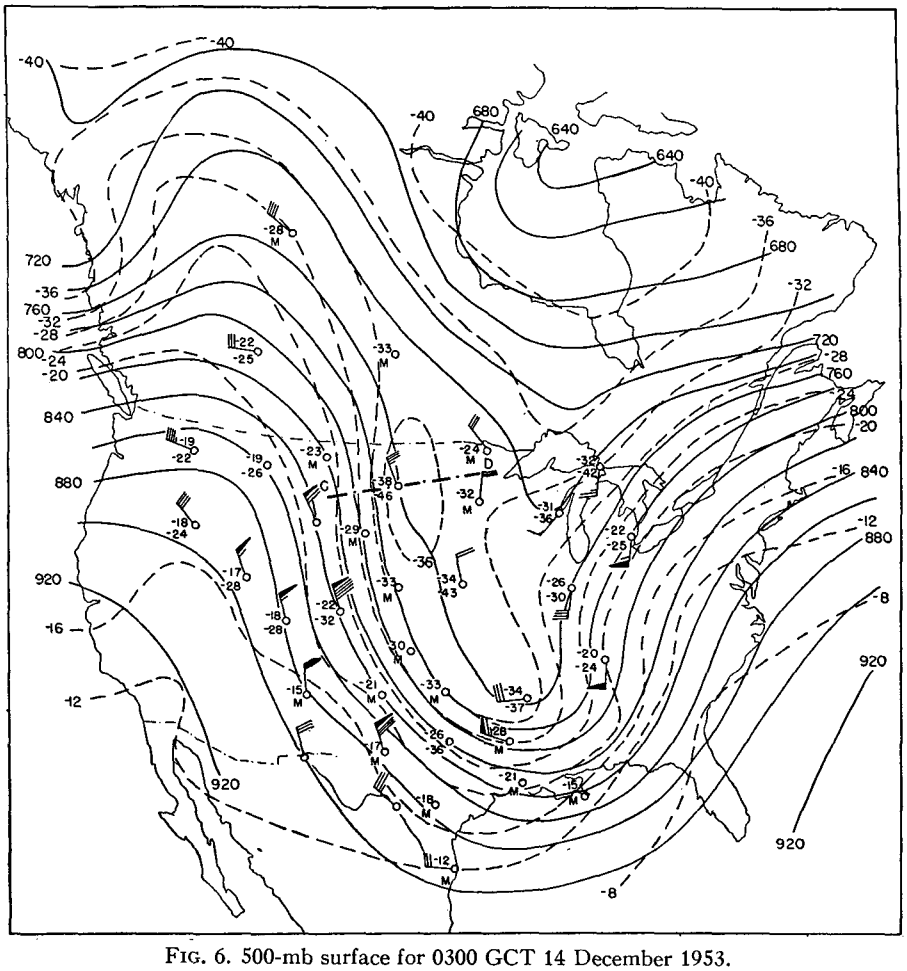

FIG. 6. 500-mb surface for 0300 GCT 14 December 1953.

development took place in the central part of the United States. Temperature gradients increased over a large area but were still of a magnitude commonly observed at the 500-mb level during the winter season. While the upper-level trough intensified only slightly during the period from 0300 GCT 14 December to 0300 GCT 15 December, the increase in temperature gradient was phenomenal (fig. 7), changing from a maximum value of 5C per 100 km to 14 C per 100 km. The boundaries of the frontal zone, and therefore the concentration of isotherms within the zone, have been determined by plotting and analyzing the pressures of the lower and upper frontal boundaries as determined from pertinent soundings. A cross section through the frontal zone indicates that the temperature gradient, as analyzed in fig. 7, is not exaggerated. This cross section and sections prepared for the two earlier times, containing roughly the same air, are shown in figs. 11 to 13. Discussion of these sections is deferred until section 5, below, because of certain unconventional features of the analyses which, to be appreciated, require a knowledge of later results.

4. Measurements and results

Measurements of potential vorticity and other significant parameters were performed on two isentropic surfaces, 300 and 310K. The 300K surface was chosen because it lay, in the final cross section, largely within the frontal zone or stable layer, entering the base of the zone near the 500-mb level and remaining within it throughout the length of the section. Most of the conclusions could be derived from a study of events on this surface alone. However, since it intersected only one frontal boundary and the origin of both is a matter of interest, it was found necessary to consider a second surface which crossed the upper boundary. For this purpose, the 310 K surface was selected.

The isentropic charts were prepared at the five synoptic hours mentioned previously. In analysis of the 300 K surface, the pressures of the 300K isentrope were read from the various soundings and plotted on regular base maps. Isobars were then drawn at 50-mb intervals. With the help of a pressure-height scale, the altitude of the isentropic surface at each wind-reporting station was next determined, and the reported vector wind at that altitude was plotted on the map. Streamlines and isotaches were drawn from these observed winds and were used to compute the "isentropic vorticity" (ζ_θ) at points on a 100-km

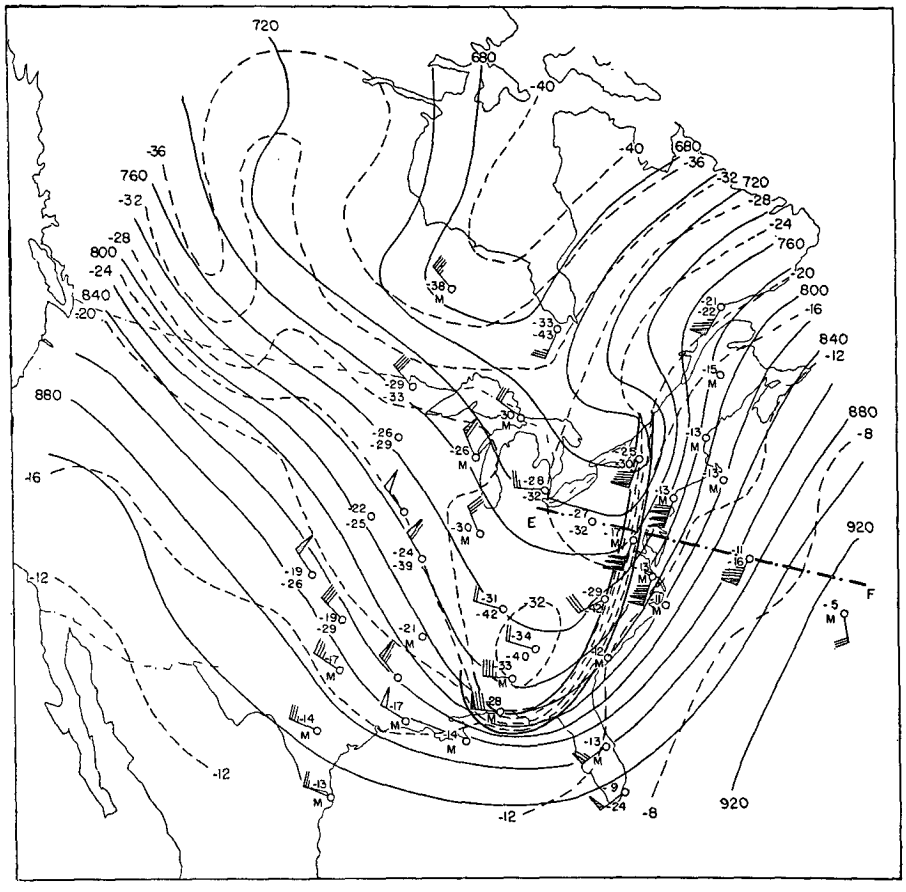

FIG. 7. 500-mb surface for 0300 GCT 15 December 1953. Heavy solid lines represent boundaries of frontal zone.

grid. The small grid distance was used to minimize the smoothing out of discontinuities in the vorticity field by the finite-difference method. A typical isentropic analysis is shown in fig. 8, except that the streamlines have been omitted for the sake of clarity.

The quantity ζ_θ at a particular grid point was next added to the appropriate value of f, the Coriolis parameter, and their sum multiplied by $\partial\theta/\partial p$ at the same point. In this way, the potential vorticity was determined over the area of the map. The stability, $\partial\theta/\partial p$, was measured from the soundings generally by taking the potential-temperature difference over a 100-mb interval surrounding the 300 K isentrope. If a significant discontinuity of lapse rate occurred within the 100-mb interval, the measurement was made over a smaller pressure range not extending beyond the discontinuity. The values of stability measured from the soundings were next plotted and analyzed, and, from the analysis, $\partial\theta/\partial p$ was interpolated at the grid points. Three of the stability charts are presented in figs. 9(a) to 9(c). The heavy solid lines in these figures denote discontinuities in $\partial\theta/\partial p$. On the earliest chart, the only important discontinuity occurs where the 300 K surface passes from the troposphere to the stratosphere; in other words, the discontinuity represents the intersection of the isentropic surface and the tropopause. At later hours, for reasons which will become apparent, the stability picture becomes

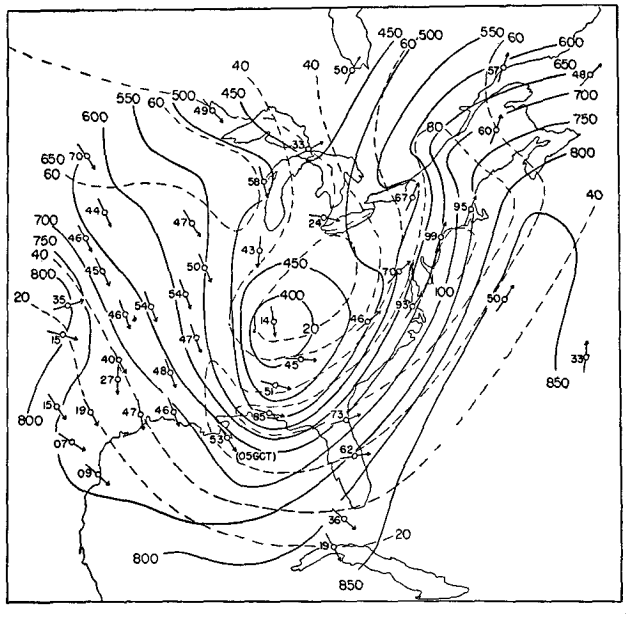

FIG. 8. 300K isentropic surface for 0300 GCT 15 December 1953, showing isobars (thin solid lines) and isotachs (thin dashed lines). Observed wind directions represented by arrows, and observed wind speeds (in knots) entered to left of stations. Pressures in millibars.

rather confused and in certain areas, indicated by broken lines, the discontinuity fades or vanishes. Where distinct, the lines of discontinuity were obtained by plotting and analyzing the potential temperatures at which major discontinuities of lapse rate appeared on the soundings.

The fields of potential vorticity on the 300 K surface are shown at 24-hr intervals in figs. 9(d) to 9(f). Since the stability field contains discontinuities, and since it can be demonstrated that the vorticity will in general be discontinuous at the thermal discontinuity, the field of potential vorticity will in general be discontinuous too. At 0300 GCT 13 December, the only discontinuity of significance is at the intersection of the 300 K surface and the tropopause. It can be seen from fig. 9(d) that this discontinuity separates high values of potential vorticity in the stratosphere from relatively low values in the troposphere. At the later hours, when the thermal structure is more complex, the potential-vorticity discontinuity can best be delineated by considering the potential-vorticity field itself.

On the basis of figs. 9(d) to 9(f), it is now possible to trace the origin of the air particles in the intense portion of the frontal zone at 0300 GCT 15 December (between 700 and 400 mb). The cross-hatching in fig. 9(*f*) indicates this region. Surprisingly enough, the potential-vorticity measurements reveal that it lies

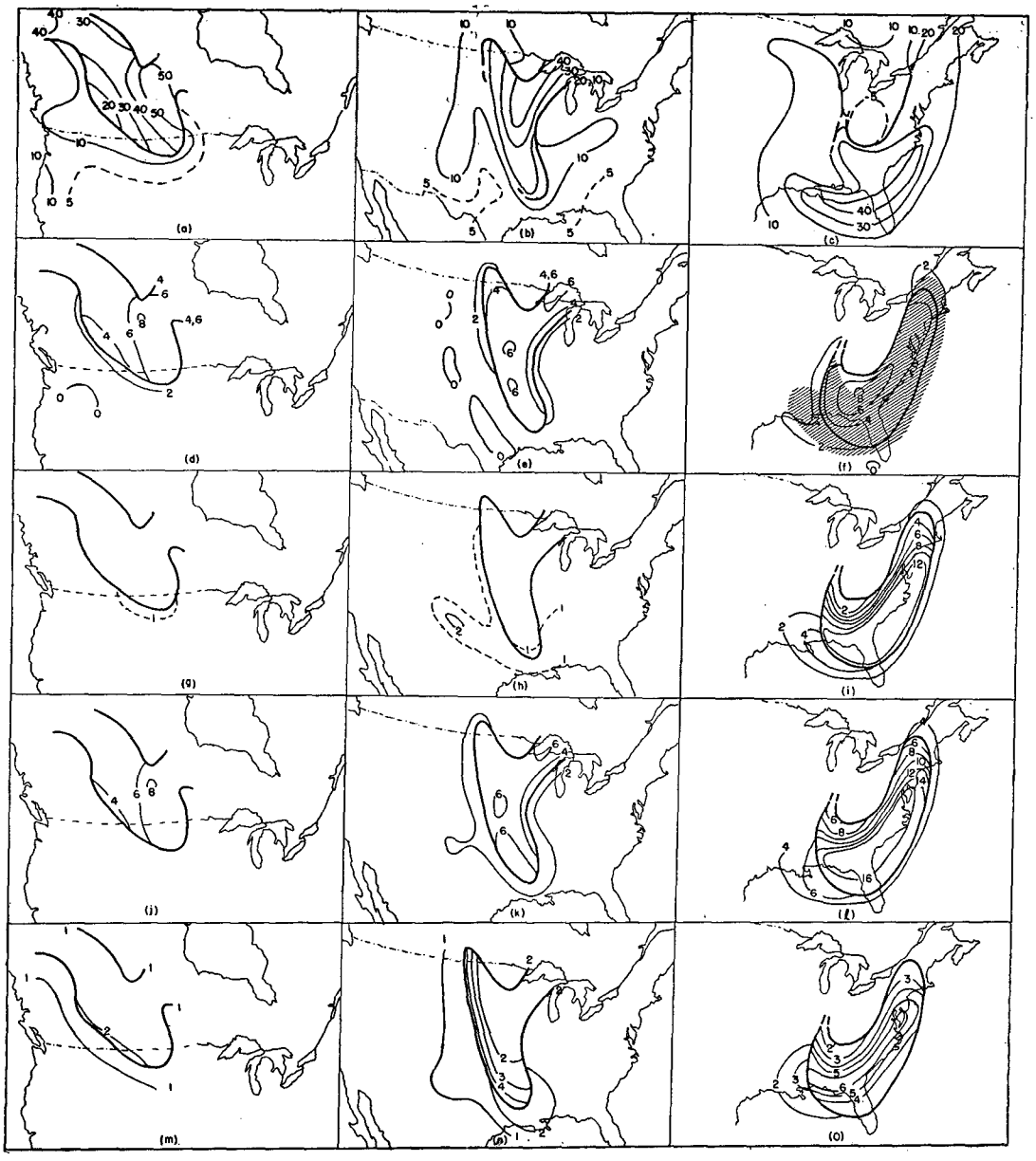

FIG. 9. a, b, c: Stability $(-\partial\theta/\partial p)$ analyses in units of deg C per 100 mb. d, e, f: Potential-vorticity $[-(\zeta_\theta + f)(\partial\theta/\partial p)]$ analyses in c.g.s. units multiplied by 10^8. g, h, i: Fields of $(RT/fp\theta)(\partial\theta/\partial n)_p^2$ in c.g.s. units multiplied by 10^8. j, k, l: Partial potential-vorticity $[-(\zeta_p + f)(\partial\theta/\partial p)]$ analyses in c.g.s. units multiplied by 10^8. m, n, o: Absolute vorticity $(\zeta_p + f)$ analyses in c.g.s. units multiplied by 10^4. All sets are for 0300 GCT 13 to 15 December 1953. On all maps, heavy solid lines represent discontinuities in pertinent quantity.

almost wholly within the area of stratospheric values; or, to state it differently, *the intense portion of the frontal zone is composed of air of stratospheric origin.* Furthermore, whereas initially the leading edge of the stratospheric air on the 300 K surface is at about 380 mb (7 km), by the final stage it has descended to about 750 mb (2½ km). This direct penetration of stratospheric air into the lower troposphere raises some interesting problems in analysis which will be resolved in subsequent paragraphs.

Now that the origin of the air in the frontal zone has been ascertained, (3) may be used, in the manner explained earlier, to study the frontal development. Under the geostrophic assumption, the second term in (3) is proportional to the square of the potential-temperature gradient. Figs. 9(g) to 9(i) give the magnitude of this term at 24-hr intervals and therefore give an indication of the growth in temperature gradient — approximately tenfold in the square of the gradient, or more than threefold in the gradient itself. The difference between this term and the potential vorticity, by (3) the partial potential vorticity, P', is depicted in figs. 9(j) to 9(l). It is interesting to note that within the frontal zone this quantity is poorly conserved. Consequently the equation expressing the conservation of partial potential vorticity, which has provided the basis of numerous studies, including recent work on numerical prediction (see Charney, 1953) does not adequately describe developments within a highly baroclinic region. By division of P' by $\partial\theta/\partial p$, the absolute vorticity, $\zeta_p + f$ is obtained. This is shown in figs. 9(m) to 9(o). Since $\zeta_p + f$ has been obtained indirectly, by the method outlined in the appendix, it must be spot-checked against directly measured values if it is to be considered an independently observed parameter. This procedure has been followed, and the agreement found to be satisfactory. The intensity of the frontogenesis in the wind field is attested to by the appearance of relative vorticities five to six times the Coriolis parameter.

On the basis of the preceding figures, the frontogenesis can now be described from both a mathematical and physical standpoint. In the initial stage (0300 GCT 13 December) the frontal air was located almost entirely within the stratosphere. The stability had characteristically high stratospheric values, and the absolute vorticity, $\zeta_p + f$, was above average but by no means abnormal. The horizontal gradient of potential temperature was rather small. During the ensuing 48-hr period, the stratospheric air subsided far into the troposphere. Similtaneously, the potential-temperature gradient underwent a large increase, and consequently the quantity $K\cdot\partial V_2/\partial p\times\nabla_p\theta$ became very large. To conserve the potential vorticity, this necessitated a correspondingly large increase of opposite sign in $(\zeta_p + f)\ (\partial\theta/\partial p)$. Since within the frontal zone as a whole $\partial\theta/\partial p$ changed little during the process, most of the change in P' is reflected in a strong rise in $\zeta_p + f$ or, more especially, ζ_p.

The exact nature of the subsidence is best understood by considering fig. 10, which shows the position of the 310 K isentrope in vertical sections normal to the flow at 24-hr intervals. The z-axis is chosen so as to contain the same air particle at the three different hours. Because of the horizontal and vertical wind shears, only this particle is in the plane of the section; but since variations are much greater across the flow than along it, the section may be thought to contain the same air particles. The frontal area ABCD is

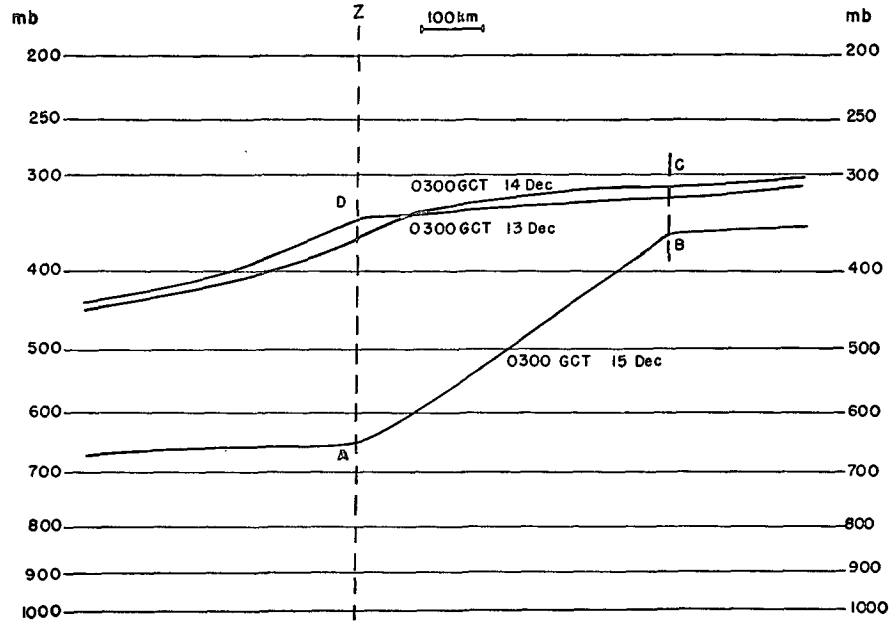

FIG. 10. Three successive positions of 310K isentropic surface in section normal to flow.

TABLE 1. Cyclonic intensity versus frontal intensity.

	Pressure at low center (mb)	$\nabla_p T$ (C per 100 km)
0300 December 13	—	4
1500 December 13	1003	5
0300 December 14	997	5
1500 December 14	982	9
0300 December 15	976	14

characterized by weakest subsidence at the cold edge and strongest subsidence at the warm, denoting an indirect solenoidal circulation. In the warm air outside the frontal zone, the circulation is direct. Thus, the diagram brings out the fact that *the increase in horizontal temperature gradient is due to a steepening of the slope of the isentropic surfaces as the result of an indirect solenoidal circulation.* In classical theory the frontal zone was regarded as the source of the solenoidal energy which, during cyclonic development, was transformed into the kinetic energy of the storm. Here it is found that the upper-level frontal zone is a dynamically produced phenomenon that intensifies as the storm intensifies, and that the circulation within it is the reverse of that required for energy release in the classical sense. Table I reveals the correspondence between the cyclone intensity at sea level and the frontal intensity at 500 mb. Moreover, no new cyclonic development of importance was observed in connection with the front after it had attained its maximum strength. These findings are in accordance with ideas already expressed by Rossby (1949) in theorizing on the mechanism of jet-stream intensification.

Another point of interest brought out by fig. 10 and various other charts is that *the frontal zone does not separate air of immediate polar and tropical origin.* Rather, it forms within the polar air-mass. Because of the strong subsidence at the warm boundary, the air at this boundary and adjacent to it on the warm side acquires temperatures characteristic of tropical air. But from the point of view of origin, it cannot be called tropical air. In a recent article, Palmén (1951) has proposed that the exchange of sensible heat in the atmosphere occurs mainly near the ground and near the tropopause, and that in the middle troposphere the polar front extends about the earth in an unbroken ring with little or no mixing of the polar and tropical air-masses. Measurements of heat flux by White (1951) do not support Palmén's thesis. The results presented here raise further doubts, since it is seen that in the present case what appears as a "polar front" separating polar and tropical air-masses is something quite different when the origin of the air is traced. At intermediate levels, where vertical motions play such an important role in determining temperature changes, it would appear preferable, unless a knowledge of the origin of the air rules to the contrary, to use the term cold and warm rather than polar and tropical.

5. The frontal boundaries

It was established in the previous section that the air within the frontal zone was of stratospheric origin. Although it is a novel idea, there is little difficulty in visualizing the tropopause subsiding to such low elevations that it appears as the lower boundary of a frontal layer. However, it is considerably more difficult to visualize how the upper boundary surface comes into existence. Initially there is only a single discontinuity surface, sloping upward to the right facing downwind. Finally there are two surfaces (excluding the tropopause) sloping in the opposite direction. Two explanations are possible:

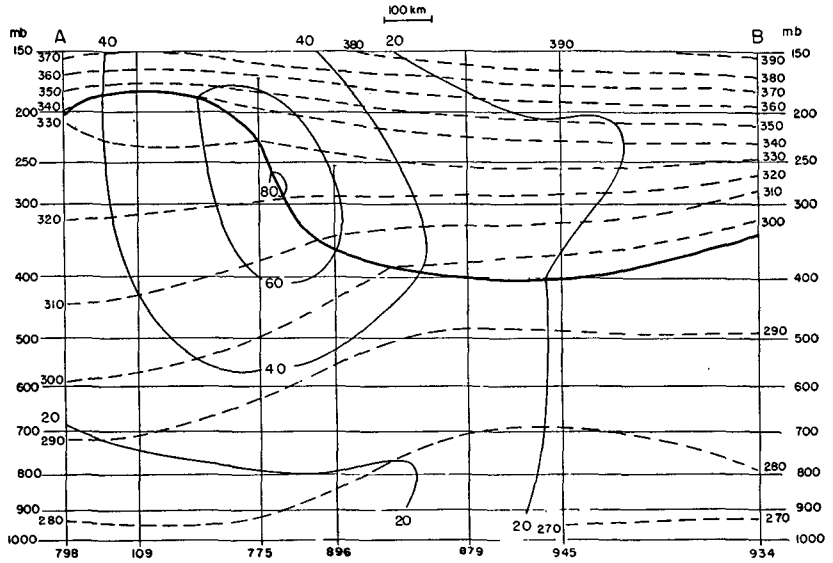

FIG. 11. Cross section along A–B in fig. 5. Thin solid lines give geostrophic wind speed (m/sec) normal to section, dashed lines are isentropes, and thick solid line represents tropopause.

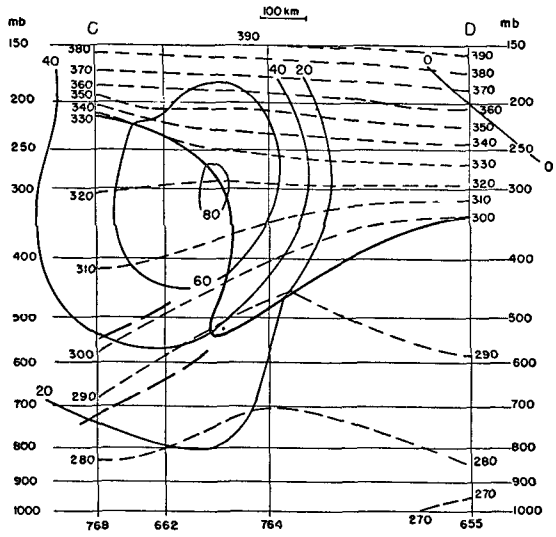

FIG. 12. Cross section along C–D in fig. 6. Heavy dashed lines represent boundaries of stable layers; otherwise notation as in fig. 11.

1. The upper surface may form in the stratospheric air during the subsidence process;
2. The tropopause may become folded, with a thin tongue of stratospheric air slicing down into the troposphere.

Since the 300 K isentrope did not intersect the warm boundary, it became necessary to consider a second and higher isentropic surface to resolve this problem. At this higher level, 310 K, the vorticity was determined from the Montgomery stream-function because of an insufficiency of actual wind data. The measurements of potential vorticity on this surface showed beyond doubt that the upper boundary of the frontal zone also separated air of distinctly tropospheric and stratospheric origin. This fact confirms alternative (2) — the folding of the tropopause — as the correct explanation of the double broundary.

With this additional piece of information, the rather unique analyses of the cross sections can now be understood. The tropopause initially was distinct and unbroken not only on the soundings used in constructing fig. 11 but also on all soundings from nearby areas, a total of 25 soundings. From fig. 11, it is apparent that the tropopause separates high stability in the stratosphere from lesser without and also, according to the wind shear along the isentropic surfaces, higher vorticity within from lesser without. Consequently the change in potential vorticity across the boundary is very large.

The section 24 hr later shows the beginning of the folding process. Simultaneously, weak stable layers, denoted by heavy broken lines in fig. 12, start to appear in the troposphere near the nose of stratospheric air. Of particular interest in this figure is the fact that, where the tropopause becomes vertical, the discontinuity in $\partial\theta/\partial p$ disappears. This accounts for the difficulty, mentioned earlier, in locating the discontinuity in the stability field at this and later hours. The discontinuities in vorticity and potential vorticity remain, however, and serve to distinguish the tropopause in the region of folding.

The final cross-section presents a picture of the stratospheric air, delineated by the heavy solid line, knifing far down into the troposphere. Conventional analysis would end the frontal boundaries near the 400-mb level and depict two separate tropopauses or perhaps multiple-tropopause structure. But what appear to be complex and unrelated discontinuity surfaces fall into a simple scheme when the initial state is known and the potential vorticity is used to trace subsequent developments.

Another unusual feature of the analysis in fig. 13 is the manner in which the frontal zone has been joined to and made continuous with a thin, dry stable layer, denoted by heavy broken lines, in the warm air-mass, while the surface cold-front is represented as a minor

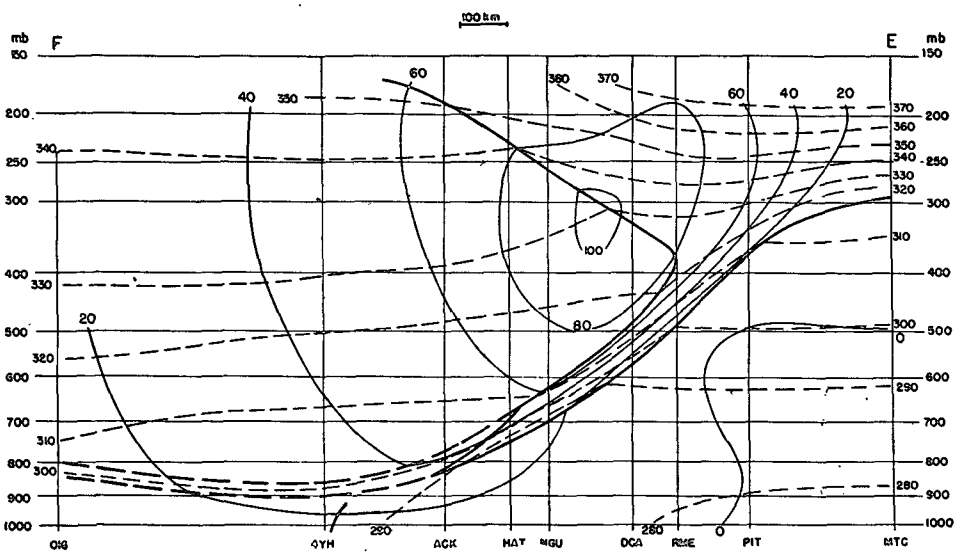

FIG. 13. Cross section along E–F in fig. 7. Notation as in figs. 11 and 12.

discontinuity, unconnected with the upper frontal zone. There were two reasons for analyzing in this fashion:

1. The stable layer in the warm air appeared to form simultaneously with the upper-level frontogenesis and within the same potential-temperature range; furthermore, the upper-level frontal zone and the surface cold-front were not initially part of the same pressure system;

2. As a check, the section was redrawn with the upper-level and surface fronts connected; this alternative analysis resulted in a greater crowding of the isotherms within the frontal zone in the vicinity of ACK and therefore in an increased thermal wind; when this thermal wind was added to the ACK wind reported at the base of the inversion (unfortunately the balloon was lost at this point), the resulting 700-mb wind velocity was well in excess of the geostrophic velocity measured from the contour spacing; no such discrepancy results from the analysis in fig. 13; Sanders (1954) has also noted the tendency for katafronts to join with a horizontal stable layer in the warm air-mass.

The development of the stable layer in the warm air-mass appears to be related, in the present instance, to the behavior of the jet stream on the 300 K isentropic surface. At the initial time, the tropopause discontinuity lay to the left of the jet axis, facing downwind; by the final it had shifted slightly to the right. Consequently, during the course of the development, air particles moved from the cyclonic to the anticyclonic side of the jet (the jet continuously reformed further and further within the cold air); to conserve potential vorticity they, of necessity, acquired greater thermal stability.

6. Summary and conclusions

The position is taken that the classical polar-front model of cyclone formation does not provide an adequate description of the structure and behavior of frontal zones in the real atmosphere and of the relationship between frontogenesis and cyclogenesis. It is proposed that the frontal problem be reexamined with recognition, first, that many so-called fronts are not fronts according to any definition involving discontinuity surfaces but are merely zones of relatively strong temperature contrast and, secondly, that, intermittently in time and space, true frontal zones do appear in the atmosphere in connection with cyclonic development. The main task of frontal theory is then to distinguish characteristic types of frontal zones and to study their origin and development.

The present study makes use of the potential vorticity on isentropic surfaces as a means of investigating one characteristic type of frontal development — the development of a katafront or sloping stable layer marked by strong vertical wind shear and rapid upward decrease in humidity. It is found in the case studied that the intense portion of the frontal zone consisted of a thin wedge of stratospheric air which had descended far into the troposphere (to 3 km or below), and that the frontal boundaries constituted a folded portion of the initial tropopause. Strongest subsidence occured at the warm boundary of the frontal zone, with little or no subsidence at the cold. During the development, stable layers tended to form in the warm air and become continuous with the protruding nose of stable stratospheric air.

The changes of absolute vorticity, stability, and horizontal potential-temperature gradient were in accordance with the Ertel vorticity theorem, the great increase in $\nabla_p\theta$ being compensated for by a large increase in vorticity. The overall change in stability was slight. In order that the various parameters of interest could be observed distinctly and measured accurately, an extremely intense case of upper-level frontogenesis was chosen for study. For this reason, it is probable that the case was unusual as regards the magnitude of the tropopause lowering. However, it is felt that this does not necessarily mean that a rare process was at work, but more likely that a common process acted with unusual intensity.

The following conclusions may be drawn from the case study:

1. The potential vorticity on isentropic surfaces (or the Ertel vorticity theorem) provides a useful tool for the study of frontogenesis;

2. The potential vorticity on pressure surfaces (partial potential vorticity) is poorly conserved in strong baroclinic zones;

3. During the formation of a katafront, or subsiding cold front, it is possible for the tropopause to become folded and for a thin slice of stratospheric air to descend to the middle or even the lower troposphere;

4. Frontal zones of the type described are the result of indirect solenoidal circulations and appear to intensify simultaneously with the surface cyclone;

5. These zones form entirely within the polar air-mass; but, because of the strong subsidence at the warm boundary, this boundary acquires temperatures characteristic of tropical air. However, it is improper to speak of such fronts as separating polar and tropical air, the designations cold and warm appearing preferable.

Acknowledgments.—The writer wishes to acknowledge that the approach to the frontal problem advocated in this article stems largely from discussions with Dr. Frederick Sanders of the Massachusetts Institute of Technology. Thanks are due Prof. James M. Austin for helpful suggestions and Miss I. Kole for assistance in the preparation of diagrams.

APPENDIX

If the potential vorticity on an isentropic surface is known from the relationship

$$P = (\zeta_\theta + f)\,\partial\theta/\partial p, \tag{2}$$

the terms

$$(\zeta_p + f)\frac{\partial\theta}{\partial p} + \boldsymbol{K}\cdot\frac{\partial \boldsymbol{V}_2}{\partial p} \times \nabla_p\theta = P \tag{3}$$

may be determined on the isentropic surface by the following approximate method.

According to the thermal wind expression,

$$\frac{\partial V_g}{\partial p} = -\frac{RT}{fp\theta}(K \times \nabla_p\theta); \tag{4}$$

so

$$K\cdot\frac{\partial V_g}{\partial p} \times \nabla_p\theta = \frac{RT}{fp\theta}\left(\frac{\partial\theta}{\partial n}\right)_p^2, \tag{5}$$

where $(\partial\theta/\partial n)_p$ is the potential-temperature gradient on a constant-pressure surface, T the temperature, and R is the gas constant.

But

$$(\partial\theta/\partial n)_p = -(\partial\theta/\partial p)(\partial p/\partial n)_\theta. \tag{6}$$

Therefore,

$$K\cdot\frac{\partial V_g}{\partial p} \times \nabla_p\theta = \frac{R}{fp}\frac{T}{\theta}\left(\frac{\partial\theta}{\partial p}\right)^2\left(\frac{\partial p}{\partial n}\right)_\theta^2. \tag{7}$$

Next, Poisson's equation in the form

$$T/p\theta = p^{\kappa-1}/p_0{}^\kappa, \tag{8}$$

where $p_0 = 1000$ mb and $\kappa = (c_p - c_v)/c_p$, may be substituted in (7) to give

$$K\cdot\frac{\partial V_g}{\partial p} \times \nabla_p\theta = \frac{R}{p_0{}^\kappa}\frac{p^{\kappa-1}}{f}\left(\frac{\partial\theta}{\partial p}\right)^2\left(\frac{\partial p}{\partial n}\right)_\theta^2. \tag{9}$$

The variables in (9) may be determined from the stability and isentropic analyses, and so the right-hand side of (9) may be evaluated from charts already prepared. Since P is known, the partial potential vorticity may be approximated by subtracting the expression in (9) from P.

REFERENCES

Bergeron, T., 1930: Über die dreidimensional verknüpfende Wetteranalyse. *Geofys. Publ.*, **5**, No. 6, 111 pp.

——, 1937: On the physics of fronts. *Bull. Amer. meteor. Soc.*, **18**, 265–275.

Bjerknes, J., 1919: On the structure of moving cyclones. *Geofys. Publ.*, **1**, No. 2, 8 pp.

——, 1932: Explorations de quelques perturbations atmospheriques à l'aide de sondages rapproachés dans le temps. *Geofys. Publ.*, **9**, No. 9, 52 pp.

——, and H. Solberg, 1926: Life cycle of cyclones and the polar front theory of atmospheric circulation. *Geofys. Publ.*, **3**, No. 1, 18 pp.

Charney, J. G., and N. A. Phillips, 1953: Numerical integration of the quasi-geostrophic equation for barotropic and simple baroclinic flows. *J. Meteor.*, **10**, 71–99.

Ertel, H., 1942: Ein neuer hydrodynamischer Wirbelsatz. *Meteor. Z.*, **59**, 277–281.

Godson, W. L., 1951: Synoptic properties of frontal surfaces. *Quart. J. r. meteor. Soc.*, **77**, 633–653.

Palmén, E., 1951: The aerology of extratropical disturbances. *Compendium Meteor.*, Boston, Amer. meteor. Soc., 599–620.

——, and K. M. Nagler, 1949: The formation and structure of a large-scale disturbance in the westerlies. *J. Meteor.*, **6**, 227–242.

Reed, R. J., and F. Sanders, 1953: An investigation of the development of a mid-tropospheric frontal zone and its associated vorticity field. *J. Meteor.*, **10**, 338–349.

Rossby, C.-G., 1949: On the nature of the general circulation of the lower atmosphere. In *The atmospheres of the earth and planets.* (G. Kuiper, ed.) Chicago, Univ. Chicago Press, 366 pp.

Sanders, F., 1954: *An investigation of atmospheric frontal zones.* (Unpubl. Sc.D. dissertation), Cambridge, Mass. Inst. Tech., 132 pp.

Sansom, H. W., 1951: A study of cold fronts over the British Isles. *Quart. J. r. meteor. Soc.*, **77**, 96–120.

Sutcliffe, R. C., 1952: Principles of synoptic weather forecasting. *Quart. J. r. meteor. Soc.*, **78**, 291–320.

White, R. M., 1951: The meridional eddy flux of energy. *Quart. J. r. meteor. Soc.*, **77**, 188–199.